Analysis and experiment of the dynamic characteristics for root-soil system in the blueberry tree

Yudong Bao*, Yuying Liu, Naifeng Yuan
(*School of Mechanical Engineering, Harbin University of Science and Technology, Harbin 150080, China*)

Abstract: To solve the problem of soil loosening caused by whole plant vibration during the operation of a vibrating blueberry harvester, the force model of the blueberry tree containing root soil was established and analyzed. The main factors affecting the impact force of the shaker were the curvature of the shaker, the branch curvature, and the equivalent elastic modulus at the impact point. Through the analysis of the transfer law of vibration between the exciting force and the root-soil complex, it is concluded that the shear strength decreases with the decrease of the internal friction angle, resulting in loose soil and easy toppling of the fruit trees. Discrete element simulation was used to analyze the force of the blueberry model. The results showed that the lower the excitation height, the more drastic the fluctuation of the root-soil complex. In the range of excitation height from 200 mm to 500 mm, soil acceleration increased by 45.5% on average for every 150 mm decrease. From 200 mm to 50 mm, the average soil acceleration increased by 69.1%. Finally, through the field excitation sensor test, the sensor was buried in 200 mm, 100 mm, and 0 mm (that is, placed on the surface) of soil, and the exciting force was applied to blueberry branches at heights of 50 mm, 200 mm, 350 mm, and 500 mm, respectively, for four times, and then the soil acceleration was output. A total of 48 sets of experimental data were obtained. By combining the scattering data obtained from the experiment with the simulated curve, it can be analyzed that when the excitation heights were 50 mm and 500 mm, the soil fluctuation at the depth of 100 mm was close to the simulated average value. When the excitation heights were 200 mm and 350 mm, the fluctuation of surface soil with a depth of 0 mm was close to the simulated average value. When the excitation height was 500 mm, the root-soil complex fluctuated twice due to the obvious reciprocating swing of the fruit tree. Since very little vibration energy was consumed during transmission, the vibration was strongest in the surface soil. Soil with a depth of 200 mm was almost unaffected by the excitation force and excitation height because too much vibration energy was consumed during transmission. The results show that the established model and simulation scheme are reliable and can provide a theoretical basis for the optimization of the incentive parameters of blueberry fruit trees.

Keywords: blueberry, fruit tree vibration, dynamic characteristics, root-soil system, experiment
DOI: 10.25165/j.ijabe.20241706.8726

Citation: Bao Y D, Liu Y Y, Yuan N F. Analysis and experiment of the dynamic characteristics for root-soil system in the blueberry tree. Int J Agric & Biol Eng, 2024; 17(6): 59–65.

1 Introduction

In recent years, China has carried out research on the key technologies of mechanized harvesting of blueberries[1,2], but the mechanized harvesting technology is still in the primary stage of research. The existing method of harvesting blueberries is vibration harvesting, but when the tree is stimulated, the roots and soil vibrate as well. If the root system is damaged, it will seriously affect the fruit ripening and yield. If the soil is seriously loose, it may cause trees to fall over and seriously affect the driving performance of the harvester. Therefore, the lack of effective matching between agricultural machinery and agronomy has been a major limiting factor for the popularity of blueberry harvesters in China.

At present, a large number of research projects on plant roots and soil vibration have been carried out at home and abroad. In these studies, the vertical displacement of the root-soil system was measured and the failure process was obtained by applying a lateral force to the trunk of the winch[3]. The interaction between soil and tools was simulated based on Coulomb's law of friction to analyze the deep burying performance and the soil loosening process[4]. In addition, fine sand containing roots was placed in a shear box for horizontal cutting to study the relationship between root deformation, diameter, and soil density[5]. The spatial distribution pattern of the root system has a significant impact on the shear strength of composite soil containing roots[6]. Through experiments, the influence of wind on root bending and the determining effect of root form distribution on plant-soil stability were studied, the relationship between soil vibration creep coefficient and vibration acceleration and its influencing factors were analyzed, and the influence of the root-soil complex on slope stability in the Qinghai spruce forest of Helan Mountain was discussed (mainly determined by soil cohesion). The pull-out resistance characteristics of shrub roots with growth period and its positive influence on slope safety factors were investigated[7-10]. The pilot model of vegetables in soil was established, and the maximum safe pallet load and maximum safe compression load of vegetable roots were obtained[11]. An improved soil-bearing settlement model was proposed, which can predict the load settlement curve based on the basic soil mechanical parameters[12]. The shear and penetration properties of simulated lunar soil under different compaction conditions were tested, and it

Received date: 2023-12-12 **Accepted date:** 2024-11-01
Biographies: Yuying Liu, MS, research interest: agricultural machinery, Email: 2192469182@qq.com; **Naifeng Yuan**, MS, research interest: agricultural machinery, Email: 752965639@qq.com.
***Corresponding author: Yudong Bao**, Professor, research interest: agricultural equipment and intelligent technology. School of Mechanical Engineering, Harbin University of Science and Technology, Harbin 150080, China. Tel: +86-0451－86390588, Email: baoyudong@hrbust.edu.cn.

was found that the shear strength increased with the increase in relative density[13]. A soil compaction model was established to provide a reference for a vegetable transplanter, and the soil load model was improved through testing and simulation, pointing out that the impact acceleration of the vehicle body should be reduced and track settlement increased[14-16]. The effects of frequency, amplitude, and excitation position (expressed as the ratio of branch action point length to total length) on coffee fruit shedding were studied[17]. The discrete element model of the root system of Panax Notoginseng was established by 3D scanning reverse modeling and EDEM software, and the simulated parameters were calibrated by physical and virtual tests[18]. The key parameters such as acceleration and velocity of berries at different frequencies were compared between simulation and experiment. The vibration transfer rate in the coffee stalk system was evaluated and the working range of selective harvesting was determined[19]. At the same time, the research method of the vibration mechanism and the separation and deformation rule of the branch-stem-fruit system of apple trees were put forward[20-21]. In addition, the studies show that the existing root-soil stability research has some limitations and cannot be fully applied to shrubs and trees, but the stability of the root-soil complex has a guiding effect on its mechanical parameters.

The objective of this study was to address the above problems by analyzing the dynamic behavior of blueberry trees and root-soil complexes during vibration harvesting. The relationship between soil porosity and root damage under different vibration frequencies was determined. The goal was to optimize the vibration parameters of vibrating blueberry harvesters to reduce negative effects on roots and soil. The specific optimization details are as follows:

Aiming at the problem of soil loosening during mechanical harvesting, and based on the biomechanical characteristics of the root system of blueberry fruit tree in the full fruiting period, a force model of the excitation force and the whole plant complex of fruit tree and root-soil was established, and its shear strength was analyzed to obtain the inertial force of soil particle vibration. Based on the discrete element method, the simulation model of soil particles and root-soil complex was established to analyze the wave mechanical behavior of soil particles under the forced vibration of fruit trees. Through a field sensing test, the acceleration of soil at different depths was analyzed, and the characteristics of the forced vibration response of the root-soil complex were studied. The mapping relationship between vibration, force, and soil loosening can be obtained, which can provide the theoretical basis for the optimization of vibration parameters of a vibrating blueberry harvester.

2 Materials and methods

2.1 Vibration analysis of blueberry tree

The frame of the blueberry picker self-moving unit adopts a "∩" type design, which guarantees the rigidity and stability of the machine. The maximum stress at full load is 53.61 MPa and the maximum displacement is 0.54 mm. The maximum stress at full load torsion is 183.24 MPa and the maximum displacement is 3.41 mm, indicating a good load ratio and torsional resistance[22]. The machine is equipped with an adjustable fruit board, which can adjust the angle according to the height of the blueberry tree to ensure that the fruit slides smoothly. During operation, the excitation frequency is set to 15-20 Hz, and the picking force is controlled between 0.3-0.5 N to ensure that only ripe fruits are picked. Finite element simulations show that when the distance between the canopy and the fruit receiving plate is 600 mm and the angle of the fruit receiving plate is 15°, the impact deformation energy of the fruit is minimal, less than 0.68×10^{-3} J, which helps to reduce the damage of the fruit[23]. During the harvesting operation, the blueberry harvester uses the excitatory effect of the exciter on the blueberry tree to make the blueberry fruit fall to the inclined fruit receiving plate and then bounce up and down to the conveyor belt. In the process, the blueberry harvester "rides" on the ridge in a straddle way. The blueberry tree passes through the harvester inside the frame. At this time, the tree will be subjected to the collision force of the exciter and the force of the fruit receiving plate (as shown in Figure 1).

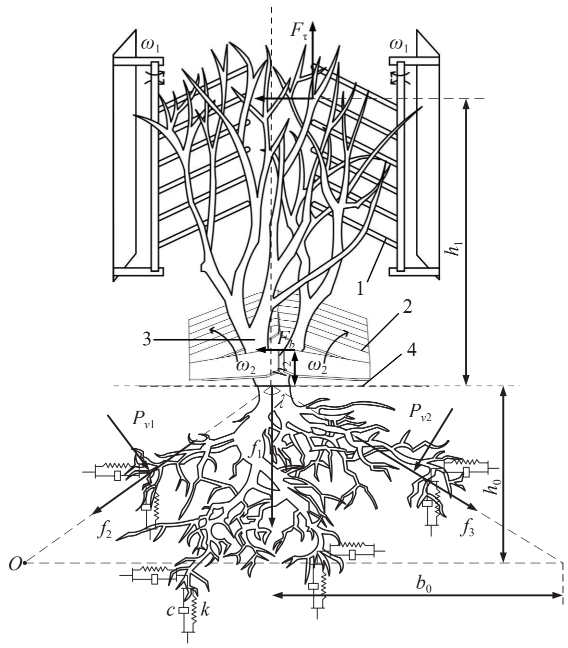

Note: 1. Vibrator 2. Fruit pickup board 3. Blueberry tree 4. Soil surface

Figure 1 Fruit pickup board operation principle

2.1.1 Fruit plate force

The force analysis of the exciter and the fruit receiving plate of the blueberry harvester is carried out by orthogonal decomposition of the collision force of the exciter into normal collision force F_a and tangential collision force F_b, which are mainly related to the exciter curvature, branch curvature, and equivalent elastic modulus at the collision point.

2.1.2 Mechanical characteristics of the root-soil complex of blueberry trees

The blueberry tree root-soil complex can be equated to a spring damping system. At the same time, the root system of trees will be hindered by soil pressure and friction[23].

According to Newton's first law, the blueberry tree and the root system are in force equilibrium under the action of external forces, and without overturning, so the blueberry root system is subject to the ultimate pulling force F_T which can be expressed as:

$$F_T = F_{f1} + \left(F_{f2} + F_{f3}\right)\cos\frac{\lambda}{2} + (P_{v1} + P_{v2})\sin\frac{\lambda}{2} \quad (1)$$

where, F_T is the ultimate pulling force on the blueberry root system, N; F_{f1} is the soil friction on the tree, N; F_{f2} is the soil friction on the left side root system, N; F_{f3} is the soil friction on the right side root system, N; P_{v1} is the soil pressure on the left side root system, N; P_{v2} is the soil pressure on the right side root system, N; λ is the angle between the root systems, °.

According to the output and torque balance equation in Figure 1, it is:

$$\begin{cases} \sum F_x = F_b + F_a + F_{f2}\cdot\sin\frac{\lambda}{2} - F_{f3}\sin\frac{\lambda}{2} - P_{v1}\cdot\cos\frac{\lambda}{2} + \\ P_{v2}\cdot\cos\frac{\lambda}{2} = 0 \\ \sum F_y = F_\tau - F_{f1} - F_{f2}\cos\frac{\lambda}{2} - F_{f3}\cos\frac{\lambda}{2} - P_{v1}\sin\frac{\lambda}{2} - \\ P_{v1}\sin\frac{\lambda}{2} = 0 \\ \sum M = P_{v1}l_1 + P_{v2}l_2 + F_{f3}l_3 + F_{f1}l_4 - F_\tau l_4 - F_a(h_1+h_0) - \\ F_b(h_2+h_0) = 0 \end{cases} \tag{2}$$

where, l_1 is the force arm of the pressure of the left root system by the soil P_{v1} to the center of rotation O, m; l_2 is the force arm of the pressure of the right root system by the soil P_{v2} to the center of rotation O, m; l_3 is the force arm of the friction force of the right root system by the soil F_{f3} to the center of rotation O, m; l_4 is the force arm of the tangential slip friction force F_τ to the center of rotation O with the friction force of the tree by the soil F_{f1}, m; h_0 is the deep burial depth of the root system, m; h_1 is the height of the shaker to the ground at the point of action of the typical collision force F_a on the blueberry tree, m; h_2 is the height of the fruit catcher plate to the floor at the end of motion of the combined force F_b on the blueberry tree, m.

The shear strength of natural soil is composed of cohesion stress and friction stress between soil particles. Thus, the shear strength of the soil τ is expressed as:

$$\tau = c + \sigma\tan\varphi \tag{3}$$

where, τ is the soil shear strength, MPa; c is the root-soil complex cohesive stress, MPa; σ is the everyday pressure, MPa; φ is the friction angle within the root-soil complex, °.

According to the Moore-Coulomb law, the shear strength τ_R of the root-soil composite is expressed as:

$$\tau_R = \tau + \tau_T \tag{4}$$

where, τ_R is the root-soil composite shear strength, MPa; τ_T is the increased root-soil composite shear strength after the reinforcement effect, MPa.

There are two growth states in the average growth of plant roots, as shown in Figure 2a. The orthogonal growth state is when the core is perpendicular to the horizontal direction in the soil. Figure 2b shows the oblique growth state, in which the root system is at a certain angle in the horizontal plane. The two states have different effects on soil reinforcement[24]. The shear strength τ'_T and τ''_T of the reinforced root-soil composite when the root system is in the orthogonal and oblique states are

$$\tau'_T = \frac{F_T}{A_2}\sin\alpha + \frac{F_T}{A_2}\cos\alpha\tan\varphi \tag{5}$$

$$\tau''_T = \frac{F_T}{A_2}\sin\left(90^\circ - \gamma\right) + \frac{F_T}{A_2}\cos\left(90^\circ - \gamma\right)\tan\varphi \tag{6}$$

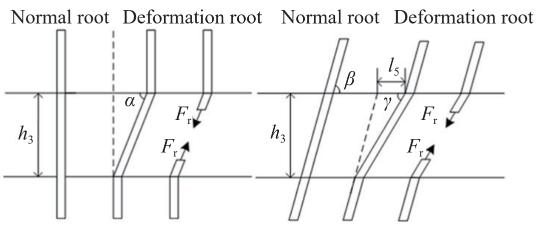

a. Orthogonal growth state b. Oblique growth status

Figure 2 Root-soil composite anchorage model

where, τ'_T is the shear strength of the reinforced root-soil composite when the root system is in the orthogonal state, MPa; τ''_T is the shear strength of the reinforced root-soil composite when the root system is in the oblique state, MPa; A_2 is the cross-sectional area of the root system, m^2; α is the angle of shear deformation when the root system is in the orthogonal state, °; γ is the angle of shear deformation when the root system is in the oblique state, °.

The shear deformation angle γ at the root system oblique cross state can be expressed as:

$$\gamma = \tan^{-1}\left[\frac{1}{\psi + \left(\tan^{-1}\beta\right)^{-1}}\right] \tag{7}$$

where, γ is the angle of shear deformation in the oblique cross state, °; β is the initial angle between the root system and the shear surface, °; ψ is the shear deformation ratio, which can be expressed as:

$$\psi = l_5/h_3 \tag{8}$$

where, l_5 is the lateral displacement of the root system after deformation in the oblique cross state, m; h_3 is the depth of the shear region, m.

The lateral displacement l_5 of the root system after deformation of the oblique growth state can be expressed as:

$$l_5 = \frac{h_3\left(\tan\beta - \tan\gamma\right)}{\tan\beta\tan\gamma} \tag{9}$$

The area of the whole root-soil complex is assumed to be A3, which includes m orthogonal root segments and n oblique root segments. Therefore, the tensile resistance of the root system is F_{T1}, $F_{T2}\ldots F_{T(m+n)}$ and the shear deformation angle of the root segment in the orthogonal growth state is α_1, $\alpha_2\ldots\alpha_m$. The initial tips between the root segment and the shear plane in the oblique growth state are $\beta_1, \beta_2\ldots\beta_n$. The corresponding shear deformation ratios are ψ_1, ψ_2 … ψ_n . Through the above analysis, it can be deduced that the shear strength τ_T of the root-soil complex increased after reinforcement. Finally, blueberry tree root-soil complex shear strength is:

$$\tau_R = \tau + \frac{\sum_{i=1}^{m} F_{Ti}\sin\alpha_i + \sum_{j=1}^{n} F_{T(m+j)}\sin\left(90^\circ - \gamma_j\right)}{A_3} + \left(\frac{\sum_{i=1}^{m} F_{Ti}\cos\alpha_i + \sum_{j=1}^{n} F_{T(m+j)}\cos\left(90^\circ - \gamma_j\right)}{A_3}\right)\tan\varphi \tag{10}$$

2.2 Study on discrete element simulation of soil wave

2.2.1 Simulation model establishment and parameter setting

The shrub roots are mostly scattered. The blueberry tree model is established according to the dispersed root morphology. The root model is set to the tertiary core, and all the main branches are equivalent to a cylinder. The soil particle model is spherical with a diameter of 1.5 mm[25].

To determine the physical characteristics of blueberry roots, several Duke blueberry roots aged six years were selected, their length and upper and lower surface diameters were measured with a Vernier caliper, the origins were equivalent to a round table, their volume was calculated, and their mass was weighed by electronic balance to obtain the density of sources. The elastic modulus of the core was determined through the tensile test. During the trial, both ends of the core were wrapped with a cotton paper towel and fine iron wire to prevent the water in the core from slipping during the tensile process. Finally, five groups of sources that completed the test were selected, and their properties are listed in Table 1. Their average density and average elastic modulus are determined as simulation parameters.

Table 1 Blueberry root system properties

	Upper surface diameter/mm	Lower surface diameter/mm	Length/ mm	Quality/ g	Density/ (kg·m^{-3})	Modulus of elasticity/ MPa
1	1.91	1.87	37.57	0.180	1644.89	1.14×10^6
2	2.57	2.35	36.20	0.225	1495.81	1.51×10^6
3	6.34	6.04	53.78	1.164	1311.82	1.01×10^6
4	5.71	5.03	15.25	0.274	1367.81	1.23×10^6
5	4.17	4.10	11.79	0.148	1426.23	1.67×10^6

During the pre-treatment, EDEM simulation parameters were set based on the blueberry root properties determined from the above trials, available data, and the GEMM material library, as listed in Table 2.

Table 2 EDEM simulation parameters

Parameters	Value
Soil particle restitution coefficient	0.600
Soil particle static friction coefficient	0.500
Soil particle dynamic friction coefficient	0.050
Restitution coefficient between soil and root	0.500
Static friction coefficient between soil and root	0.700
Dynamic friction coefficient between soil and root	0.150
Poisson's ratio of roots	0.394
Modulus of elasticity of the root	1.31×10^6
Root density	1449.31 kg·m^{-3}

2.2.2 Simulation scheme design

Firstly, a soil trough was established in EDEM, the trees were introduced into the soil trough, and then soil particles were generated to completely cover the root system of the trees, forming a root-soil complex.

Taking the three-stage root end, i.e., depth h_0=250 mm, as the center of rotation, 50 mm, 200 mm, 350 mm, and 500 mm were chosen as different excitation heights. Then, 50-500 N of force was applied with a spacing of 50 and the corresponding torque 10 times. In the simulation process, the time step was set to 5%, with a data storage interval of 0.1 s and a simulation time of 1 s. Finally, 40 groups of simulation data were obtained.

2.3 Field experiments

To verify the mapping relationship between the excitation force and the fluctuation of the root-soil complex, a knocking test was carried out on Duke blueberry trees aged six years in the Horticulture Branch of Heilongjiang Academy of Agricultural Sciences in late July 2021 using the Dh5922 acquisition box (Dong Hua, China), PCB acceleration sensor (Dong Hua, China), Dong Hua hand-held impact hammer (Dong Hua, China), shaker (self-made), and Dong Hua DHDAS dynamic signal acquisition and analysis system (Dong Hua, China). This equivalently replaced the contact collision and excitation effects of the harvester on the trees in field harvesting operations. Figure 3 shows the test equipment and the vibration picking test rig.

Percussion tests were first carried out according to the EDEM simulation scheme, and four excitation heights of 50 mm, 200 mm, 350 mm, and 500 mm were also selected for the impact hammer strike tests. To obtain the vibration of the root-soil complex at different depths, accelerometers (Dong Hua, China) were fixed to the root system and to the soil at depths of 200 mm, 100 mm, and 0 mm (that is, at the soil surface). Multiple strikes were performed at each test condition. Valid test values for four instantaneous accelerations of the root-soil complex were obtained. Finally, suitable excitation frequencies of 120 r/min, 150 r/min, and 180 r/min were selected for the excitation test. At this point, the sensors were also fixed to the root system at depths of 200 mm, 100 mm, and to the soil surface (depth of 0 mm). The combined acceleration of all test data represents the fluctuations at different depths within the root-soil complex at different excitation frequencies. Table 3 lists the scheme of the simulation test.

Table 3 The scheme of simulation test

Serial number	Shaker excitation frequency/r·min^{-1}	Depth of sensor burial/mm	$\bar{a}$/(m·s^{-2})
01	120	0	17.425
02	120	100	7.238
03	120	200	1.814
04	150	0	18.122
05	150	100	7.765
06	150	200	3.072
07	180	0	18.687
08	180	100	8.982
09	180	200	4.193

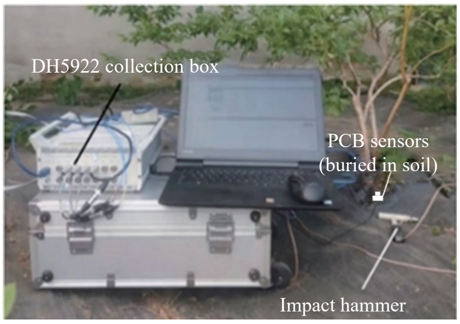

a. Test equipment

b. Vibratory picking test rig

Figure 3 Tree excitation test

3 Results and discussion

After the blueberry trees are excited by the harvester, the soil will fluctuate and the internal friction angle of the root-soil complex and its surrounding soil will decrease. At the same time, the shear strength of the root-soil complex will decrease with the decrease of the internal friction angle, resulting in the loosening of the soil and the overturning of the trees.

The inertial force of soil particles when they fluctuate is mainly affected by acceleration. This article uses the average output speed to represent the fluctuation level. Figure 4a-4d respectively show the fluctuation degree of the root-soil complex acceleration with the excitation heights of 50 mm, 200 mm, 350 mm, and 500 mm when

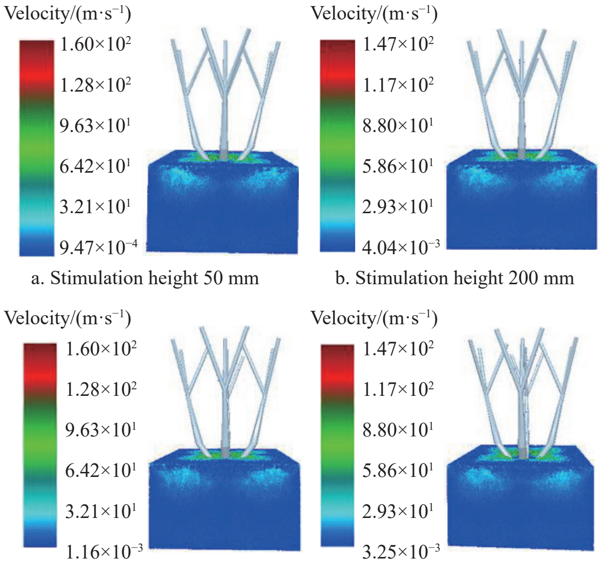

a. Stimulation height 50 mm b. Stimulation height 200 mm

c. Stimulation height 350 mm d. Stimulation height 500 mm

Figure 4 Velocity fluctuation of root-soil composite with excitation force of 50 N

the excitation force is 50 N. It can be seen that the topsoil has the maximum velocity. The velocity of the ground in contact with the roots in the root-soil complex is relatively large. The higher the position of excitation, the lower the overall fluctuation level of the root-soil complex.

All the data is fitted into the *F-a* curve to obtain the relationship between the excitation force and the instantaneous acceleration of the root-soil complex. Figure 5 shows the *F-a* fitting curve under four different excitation heights.

The scatter data from the force hammer impact test was put into the *F-a* curve obtained by fitting the simulation to get Figure 6.

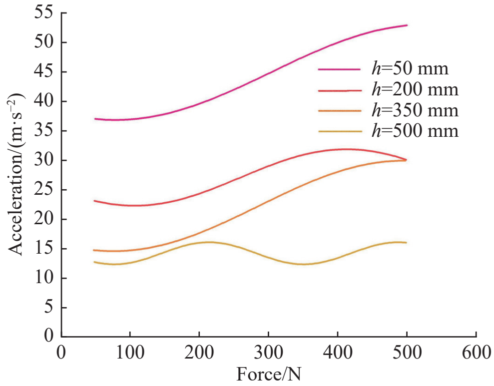

Figure 5 *F-a* fitting curve

It can be seen from Figure 6 that in the four excitation height tests, the soil at a depth of 200 mm was at the end of the root-soil complex, and the excitation force had little effect on the earth. When the excitation height was 50 mm, the loss of vibration energy in the process of transmission to the soil was slight, so the fluctuation degree of the surface soil was the largest. At this same excitation height of 50 mm, for the soil at a depth of 100 mm, the fluctuation degree was close to the average simulation value. When the excitation heights were 350 mm and 500 mm, the overall fluctuation level of the root-soil complex decreased.

As shown in Figure 7, the first acceleration fluctuation was the effect of the impact hammer, and the second acceleration fluctuation was caused by the swing of trees after being excited.

After processing the shaker excitation test data using Origin, the fluctuation curves for the complete root-soil complex under shaker action were obtained, as shown in Figure 8.

According to Figure 8, under the action of three different excitation frequencies, the root-soil composite surface fluctuated the

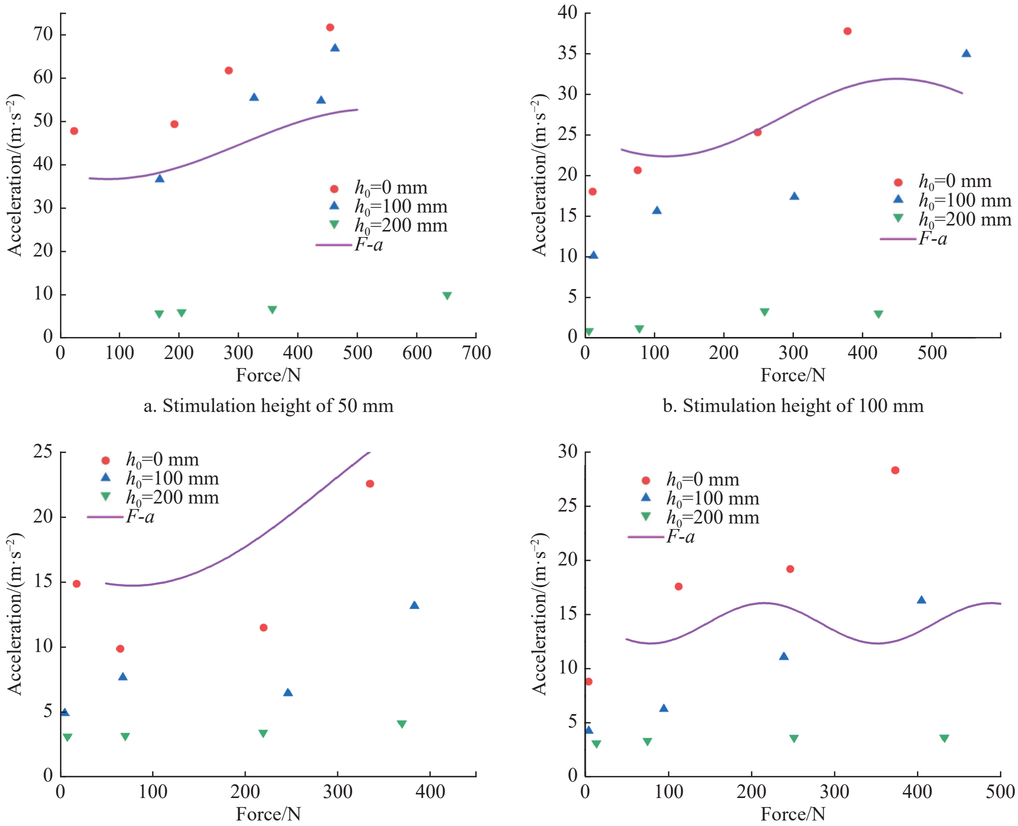

a. Stimulation height of 50 mm b. Stimulation height of 100 mm

c. Stimulation height of 350 mm d. Stimulation height of 500 mm

Figure 6 Acceleration fluctuation level of the root-soil complex

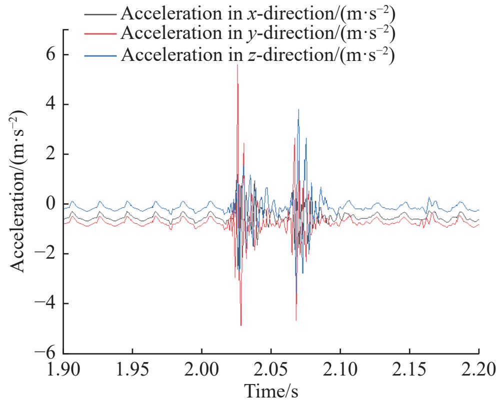

Figure 7 Acceleration of excitation (height 500 mm/depth 100 mm)

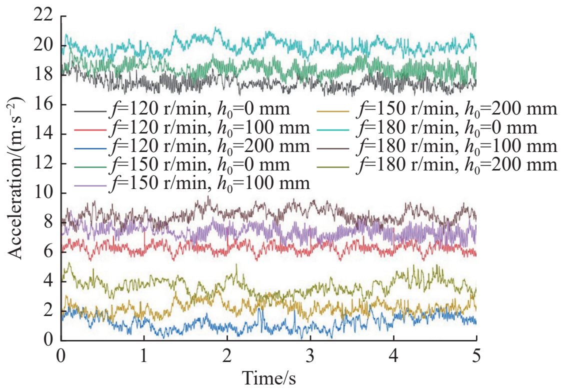

Figure 8 Fluctuation curves of root-soil complexes under excitation

most at a depth of 0 mm, with acceleration in the range of 17-22 m/s². The acceleration range at a depth of 100 mm was in the range of 5-10 m/s². At a depth of 200 mm, the fluctuations were the smallest, with accelerations in the range of 0-5 m/s². In addition, the acceleration magnitude of the root-soil composite at each excitation frequency was 0 mm>100 mm>200 mm in depth.

Based on the position of the blueberry fruit tree about the shaker, it can be seen that the center of the crown is close to the height of the fruit tree at 500 mm. Therefore, for the analysis of the acceleration of the root-soil complex under the action of the shaker, the situation in Figure 6d is considered. At a depth of 200 mm, the root-soil complex fluctuation level was low in both the percussion and excitation tests and had little effect on the results of the study. Therefore, the data at a depth of 200 mm was not considered in the analysis. The acceleration of the root-soil complex under the action of the shaker was also combined with Figure 6d to obtain Figure 9 and then analyzed.

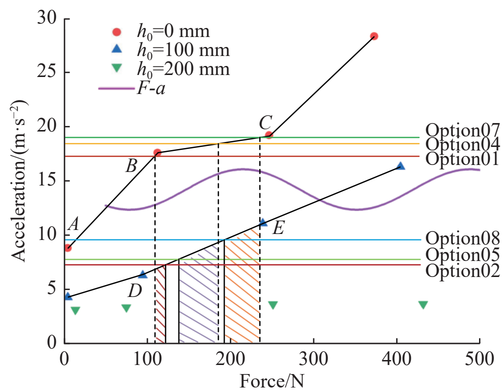

Figure 9 Relationship between percussion test and excitation test

When a blueberry harvester is in operation, the shaker exerts a continuous vibration on the fruit tree. According to Figure 9, the force on the soil surface at each excitation frequency and a depth of 100 mm is taken as the range of excitation forces in that excitation frequency. The excitation frequency of the shaker is 120 r/min, and the force of the blueberry tree is 110.84-123.97 N. At 150 r/min, the force of the blueberry tree is 139.94-156.08 N. At 180 r/min, the force of the blueberry tree is 176.82-203.17 N.

4 Conclusions

To solve the problem of soil loosening caused by the vibration of fruit trees during the operation of the existing vibrating blueberry harvester in China, the relationship between the excitation force and the soil fluctuation of the root-soil complex was quantitatively studied by combining theory, simulation, and experiment.

1) Based on the principle of vibration picking, the mechanical behavior of the root-soil complex of blueberry fruit trees after excitation was established, and the evolution law model and response relationship between the excitation force and the vibration transmission of fruit trees and root-soil complexes were established. It was found that after the blueberry fruit trees were excited by the harvester, the soil would fluctuate, the internal friction angle of the root-soil complex and its surrounding soil would decrease, and its shear strength would decrease with the decrease of the internal friction angle, resulting in soil loosening and fruit trees being prone to overturning.

2) Based on the discrete element method, the wave dynamics behavior of the root-soil complex and soil particles under forced vibration of fruit trees was analyzed. It was found that the lower the excitation height, the more severe the fluctuation of the root-soil complex. When the excitation height was 50 mm, the acceleration of the root-soil complex was significantly higher than it was at the other three excitation heights. At the excitation heights of 500 mm, 350 mm, and 200 mm, the soil acceleration increased by 45.5% for every 150 mm decrease. When the excitation height was reduced from 200 mm to 50 mm, the average soil acceleration increased by 69.1%.

3) Through field tests, it is found that when the excitation height was 50 mm, the soil acceleration with a depth of 100 mm was close to the simulated average. When the excitation heights were 200 mm and 350 mm, the acceleration of the surface soil was close to the simulated value. When the excitation height was 500 mm, the soil acceleration with a depth of 100 mm was close to the simulated value, and the soil produced secondary fluctuations. Soils at a depth of 200 mm were almost unaffected by the excitation force and excitation height.

This study on the influence of blueberry harvester operation on the root-soil complex of blueberry fruit trees has determined the mapping relationship between excitation force and soil loosening, which can provide a reference for obtaining the threshold of forced vibration lodging of fruit trees, thus avoiding the overturning phenomenon of fruit trees due to unsuitable operating parameters, and help to improve the driving safety of harvesters. This will provide theoretical guidance and practical value for the improvement of the mechanization level of small berry harvesting operations in China.

Acknowledgements

This work was supported by Heilongjiang Provincial Discipline Collaborative Innovation Achievement Project (Grant No. LJGXCG2022-075) and Postdoctoral Scientific Research Developmental Fund of Heilongjiang Province (LBH-Q21020).

[References]

[1] Zhang C Q, Wang Q, Huang Z J, Wu W L, Li G P, Li W L. Development and prospect of blueberry industry in Jiangsu Province. Northern Horticulture, 2021; 9(18): 155–160. (in Chinese)

[2] Bao Y D, Yang C, Zhao Y L, Liu X L, Guo Y L. Collision injury assessment of mechanical harvesting blueberry fruit based on collision deformation energy. Transactions of the CSAE, 2017; 33(16): 283–292. (in Chinese)

[3] Coutts M P. Components of tree stability in sitka spruce on peaty gley soil. Forestry, 1986; 59(2): 173–197.

[4] Mouazen A M, Neményi M. Finite element analysis of subsoiler cutting in non-homogeneous sandy loam soil. Soil and Tillage Research, 1999; 51(1-2): 1–15.

[5] Abe K, Ziemer R R. Effect of tree roots on a shear zone: modeling reinforced shear stress. Canadian Journal of Forest Research, 1991; 21(7): 1012–1019.

[6] Kong G Q, Wen L, Liu H L, Wang C Q. Strength properties of root compound soil and morphological observation of plant root. Rock and Soil Mechanics, 2019; 40(10): 3717–3723.

[7] Deans J D, Ford E D. Modelling root structure and stability. Plant and Soil, 1983; 71: 189–195.

[8] Rasulov H Z, Rasulov R H, Tashxodjayev A U, Babajanov M B. Vibration creep of loess soils. IOP Conference Series: Earth and Environmental Science, 2020; 614: 012064.

[9] Tian J, Ji J N, Zhong Q, Yu P C, Yang L J, Yang B. Analysis on the improvement of slope stability in root-soil composite of Picea crassifolia forest in Helan Mountain. Transactions of the CSAE, 2017; 33(20): 144–152. (in Chinese)

[10] Zheng M X, Huang G, Peng J. Tensile-pullout properties of roots of Magnolia multiflora in different growth stages and stability of slope with its root. Transactions of the CSAE, 2018; 34(20): 175–182. (in Chinese)

[11] Gao G H, Xie H F, Wang T B. EDEM simulation and experiment of pullout force of protected vegetable harvester. Transactions of the CSAE, 2017; 33(23): 24–31. (in Chinese)

[12] Zhao J F, Wang W, Sun Z X, Su X J. Improvement and verification of pressure-sinkage model in homogeneous soil. Transactions of the CSAE, 2016; 32(21): 60–66. (in Chinese)

[13] Huang H, Wu B G, Xu S C, Zou M, Li J Q, Li J H. Test study on mechanical properties of lunar soil simulant under high compactness condition. Transactions of the CSAE, 2019; 35(1): 31–38. (in Chinese)

[14] Yang S H, Song L, Jia X P, Xie S Y. Research and test on vibration compaction of duckbilled planter of vegetable transplanter. Journal of Agricultural Mechanization Research, 2021; 43(3): 201–206, 214. (in Chinese)

[15] He J, Wu D L, Ma J S, Feng W X, Wang H K. A study on travel vibration characteristics of tracked vehicle based on improved soil pressure-sinkage model. Journal of Vibration and Shock, 2020; 39(12): 57–62, 77. (in Chinese)

[16] Zhang W H, Wang G Y, Hu S H, Zhang Y J, Quan P, Chang J M. Indoor experimental study on the pull-out force of Symplocos anomala brand root. Science of Soil and Water Conservation, 2020; 18(3): 22–30. (in Chinese)

[17] Yu Y J, Cao Y, Lai Q H, Zhao Q H, Sun Z X, Zhou S W, et al. Design and operation parameters of vibrating harvester for Coffea *arabica* L. Agriculture, 2023; 13(3): 700.

[18] Xie K T, Zhang Z G, Wang F A, Yu X L, Wang C L, Jiang S F. Calibration and experimental verification of discreteelement parameters of Panax notoginseng root. Int J Agric & Biol Eng, 2024; 17(4): 13–23.

[19] Yan D, Luo L F, Zhang P, Liu W T, Wang J X, Lu Q H, et al. Vibration analysis and experimental study of the effects of mechanised grape picking on the fruit - stem system. Biosystems Engineering, 2023; 227: 82–94.

[20] Villibor G P, Santos F L, Queiroz D M, Khoury Junior J K, Pinto F A C. Vibration transmissibility of the coffee fruit-peduncle system: A forced vibration study of high frequency aiming mechanical harvesting. Engenharia Agrícola, 2023; 43(1).

[21] Sun X D, Wu W D, Cao C M, Xu L X, Jiang R, Fang L F, et al. Research on vibration response characteristics and separation deformation law of fruit-branch system. AIP Advances, 2023; 13(6): 1–9.

[22] Bao Y D, Liang Z, Zhao Y L, Liu X L, Yang J, Guo Y L, et al. Design and performance of high-throughput self-propelled device for blueberry harvester. Transactions of the CSAE, 2018; 34(24): 36–45. (in Chinese)

[23] Bao Y D, Yang C, Zhao Y L, Liu X L, Guo Y L. Vibration characteristics analysis and experiment of the blueberry shrub. Journal of Harbin University of Science and Technology, 2018; 23(1): 18–22. (in Chinese)

[24] Shi D Q, Zhao L T, Zhang X. The technology of slope protection by vegetation in slope ecological protection engineering. Journal of Inner Mongolia Forestry Science and Technology, 2012; 38(1): 56–58.

[25] Bao Y D, Yang J, Zhao Y L, Liu X L, Guo Y L, Li Z P. Design of the walking driving system for a blueberry harvester based on contact mechanical behavior of wheel-soil. Transactions of the CSAE, 2020; 36(7): 43–52.